

**NASA TECHNICAL  
MEMORANDUM**

**NASA TM X- 72825**

**NASA TM X- 72825**

(NASA-TM-X-72825) IMPROVED STRESS-INTENSITY  
FACTORS FOR SEMI-ELLIPTICAL SURFACE CRACKS  
IN FINITE-THICKNESS PLATES (NASA) 31 p HC  
103/MF A01 CSCL 20K

**N77-27427**

**G3/39 Unclas  
29151**

**IMPROVED STRESS-INTENSITY FACTORS FOR SEMI-ELLIPTICAL  
SURFACE CRACKS IN FINITE-THICKNESS PLATES**

by  
I.S. Raju and J.C. Newman, Jr.  
Langley Research Center  
Hampton, VA 23665

**TECHNICAL PAPER to be presented at the 4th International Conference  
on Structural Mechanics in Reactor Technology, August 15 - 19, 1977,  
San Francisco, California, U.S.A.**

This informal documentation medium is used to provide accelerated or  
special release of technical information to selected users. The contents  
may not meet NASA formal editing and publication standards, may be re-  
vised, or may be incorporated in another publication.

**NATIONAL AERONAUTICS AND SPACE ADMINISTRATION  
LANGLEY RESEARCH CENTER, HAMPTON, VIRGINIA 23665**





IMPROVED STRESS-INTENSITY FACTORS FOR SEMI-ELLIPTICAL  
SURFACE CRACKS IN FINITE-THICKNESS PLATES

I. S. Raju and J. C. Newman, Jr.  
NASA-Langley Research Center  
Hampton, Virginia

SUMMARY

Surface cracks are among the more common flaws in aircraft and pressure vessel components. Accurate stress analyses of surface-cracked components are needed for reliable prediction of their crack-growth rates and fracture strengths. Several calculations of stress-intensity factors for semi-elliptical surface cracks subjected to tension have appeared in the literature. However, some of these solutions are in disagreement by 50 to 100 percent.

In this paper stress-intensity factors for shallow and deep semi-elliptical surface cracks in plates subjected to tension are presented. To verify the accuracy of the three-dimensional finite-element models employed, convergence was studied by varying the number of degrees of freedom in the models from 1500 to 6900. The 6900 degrees of freedom used here were more than twice the number used in previously reported solutions.

## INTRODUCTION

Surface cracks are among the more common flaws in aircraft and pressure vessel components. Accurate stress analyses of these surface-cracked components are needed for reliable prediction of their crack-growth rates and fracture strengths. Exact solutions to these difficult problems are not available; therefore, approximate methods must be used. For a semi-elliptical surface crack in a finite-thickness plate subjected to tension (Figure 1), Browning and Smith [1], Kobayashi [2], and Smith and Sorensen [3] used the alternating method and Kathiresan [4] used the finite-element method to obtain the stress-intensity factor variations along the crack front for various crack shapes. For a deep semi-elliptical surface crack (with  $a/t = 0.8$  and  $a/c = 0.2$ ) subjected to tension, the stress-intensity factors obtained by Smith and Sorensen [3], Kobayashi [2], and Kathiresan [4] disagreed by 50 to 100 percent. The reasons for these discrepancies are not well understood.

This paper presents stress-intensity factors for shallow and deep semi-elliptical surface cracks in plates subjected to uniform tension. To test the validity of the present analysis, two crack configurations, both embedded in a large body subjected to uniform tension, were analyzed: (1) a circular (penny-shaped) crack and (2) an elliptical crack. These results are compared with exact solutions from the literature [5]. To verify the accuracy of the solutions for surface cracks in finite-thickness plates, convergence was studied by varying, from 1500 to 6900,

the number of degrees of freedom in the finite-element models. The 6900 degrees of freedom used here were more than twice the largest number used previously [4]. These models were composed of singular elements around the crack front and isoparametric (linear strain) elements elsewhere. Mode I elastic stress-intensity factors were calculated by using a nodal force method.

The computations reported herein were conducted on a unique computer called the STAR-100 at the NASA Langley Research Center.

SYMBOLS

|        |   |
|--------|---|
| a      | depth of surface crack                      |
| b      | half-width of cracked plate                 |
| c      | half-length of surface crack                |
| E      | Young's modulus of elasticity               |
| F      | stress-intensity boundary-correction factor |
| h      | half-length of cracked plate                |
| K      | stress-intensity factor (Mode I)            |
| Q      | shape factor for an elliptical crack        |
| S      | applied uniform stress                      |
| t      | plate thickness                             |
| x,y,z  | Cartesian coordinates                       |
| $\nu$  | Poisson's ratio                             |
| $\phi$ | parametric angle of the ellipse             |

### THREE-DIMENSIONAL ANALYSIS

Several attempts [6-8] have been made to develop special three-dimensional finite-elements that account for the stress and strain singularities caused by a crack. These elements have had assumed displacement or stress distributions that simulate the square-root singularity of the stresses and strains at the crack front. Such three-dimensional singularity elements [9] were also used herein for the analysis of finite-thickness plates containing embedded elliptical or semi-elliptical surface cracks (see, for example, Figure 1).

#### Finite-Element Idealization

Two types of elements (isoparametric and singular) [9] were used in combination to model elastic bodies with embedded elliptical cracks or semi-elliptical surface cracks. Figure 2 shows a typical finite-element model for an embedded circular crack in a large body ( $h/a = b/a = 5$ ). This model idealizes one eighth of the body. Various numbers of wedges were used to form the desired configuration. Figure 2(a) shows a typical model with eight wedges. Each wedge is composed of elements that are identical in pattern to that shown in the  $\phi = \text{constant}$  plane. The arrangement of the elements around the crack front is shown in Figure 2(b). The isoparametric (linear strain) elements (denoted as I) were used everywhere except near the crack front. Around the crack front each wedge contained eight "singularity" elements (S) in the shape of pentahedrons. The "singularity" elements

had square-root terms in their assumed displacement distribution and, therefore, produced a singular stress field at the crack front. Details of the formulation of these types of elements are given in Reference 9.

The finite-element model for the embedded elliptical or semi-elliptical surface crack was obtained from the finite-element model for the circular crack by using an elliptic transformation. This transformation was needed because the stress-intensity factors must be evaluated from either crack-opening displacements or nodal forces along the normals to the crack front. If  $(x,y,z)$  are the Cartesian coordinates of a node in the circular-crack model and  $(x',y',z')$  are the coordinates of that same node in the elliptical-crack model, then the transformation is given by

$$\begin{aligned}x' &= x \sqrt{1 + \frac{c^2 - a^2}{x^2 + z^2}} \\y' &= y\end{aligned}\tag{1}$$

and

$$z' = z$$

for  $x$  and  $z$  not at the origin. Figure 3 shows how circular arcs and radial lines in the  $x,z$  plane of the circular-crack model are transformed into ellipses and hyperbolas, respectively, in the  $x',z'$  plane of the elliptical-crack model using equations (1). Because equations (1) are not valid at the origin, a circle of very small radius,  $a/1000$ , was used near the origin in the circular crack model. The small circle maps onto an extremely narrow ellipse in the  $x',z'$  plane. The use of

the small circle avoids ill-shaped elements near the origin in the elliptical-crack model. Figure 4 shows a typical finite-element model of a finite plate containing an elliptical crack. The transformation reduced the b/c ratio; therefore, in order to maintain  $b/c \geq 4$ , additional elements were added along the x'-axis to eliminate the influence of plate width.

#### Stress-Intensity Factor

The stress-intensity factor is a measure of the magnitude of the stresses near the crack front. Under general loading, the stress-intensity factor depends on three basic modes of deformation (tension and in- and out-of-plane shear). But here only tension loading was considered and, therefore, only Mode I deformations occurred. The Mode I stress-intensity factor, K, at any point along an elliptical or semi-elliptical crack in a finite plate is taken to be

$$K = S \sqrt{\pi \frac{a}{Q}} F\left(\frac{a}{t}, \frac{a}{c}, \phi\right) \quad (2)$$

where S is the applied stress, a is the crack depth, Q is the shape factor for an ellipse and is given by the square of the complete elliptic integral of the second kind [5]. The boundary-correction factor,  $F(a/t, a/c, \phi)$ , is a function of crack depth, crack length, plate thickness and the parametric angle of the ellipse. The present paper gives values for F as a function of a/t and  $\phi$  for  $a/c = 0.2$  and 1.0. The a/t values ranged from 0.2 to 0.8.

The stress-intensity factors from the finite-element models of embedded elliptical and semi-elliptical surface cracks were obtained by using a nodal force method, details of which are given in Reference 9. In this method, the nodal forces normal to the crack plane and ahead of the crack front are used to evaluate the stress-intensity factor. In contrast to the crack-opening displacement method [6], this method requires no prior assumption of either plane stress or plane strain. For a surface crack in a finite plate, the state of stress varies from plane strain in the interior of the plate to plane stress at the surface. Thus, the crack-opening displacement method could yield erroneous stress-intensity factors.

#### RESULTS AND DISCUSSION

In the following sections a circular (penny-shaped) crack and an elliptical crack completely embedded in a large body subjected to uniform tension were analyzed using the finite-element method. The calculated stress-intensity factors for these crack configurations are compared with the exact solutions to verify the validity of the present finite-element method.

For a semi-circular and semi-elliptical surface crack in a finite-thickness plate, convergence of the stress-intensity factors was studied while the number of degrees of freedom in the finite-element models ranged from about 1500 to 6900. The stress-intensity factor variations along the crack front for semi-circular ( $a/c = 1$ ) and semi-elliptical

( $a/c = 0.2$ ) surface cracks were obtained as functions of  $a/t$  with  $h/c = b/c \geq 4$ . Whenever possible, these stress-intensity factors are compared with results from the literature.

#### Exact Solutions

In this section a comparison is made between the stress-intensity factors calculated from the finite-element analysis and from the exact solution [5] for an embedded circular (penny-shaped) crack ( $a/c = 1$ ) and an embedded elliptical crack ( $a/c = 0.2$ ) in an infinite body. In the finite-element model,  $h$  and  $b$  were taken to be large enough that the free boundary would have a negligible effect on stress intensity. The boundary correction on stress intensity for a circular crack in a cylinder of radius  $b$  with  $b/a = 5$  is about one percent [10]. Therefore, to simulate a large body the finite-element model was assigned the dimensions  $h/a = b/a = 5$ , along with 3078 degrees of freedom. The calculated stress-intensity factors along the crack front from the circular crack model were about 0.4 percent below the exact solution.

The embedded elliptical crack ( $a/c = 0.2$ ) model, with  $h/c = h/c = 4$  and  $t/a = 5$ , had 3348 degrees of freedom. The influence of finite boundaries on stress intensity was estimated to be about one percent. The finite-element analysis gave stress-intensity factors along the crack front generally within one percent of the exact solution, except in the region of sharpest curvature of the ellipse, where the calculated values were about 3 percent higher than the exact solution. Further refinement in the mesh size in this area gave more accurate stress-intensity factors.

Because the present method yielded stress-intensity factors for completely embedded circular and elliptical cracks within 0.4 to 3 percent of the exact solutions, the method was considered suitable for analyses of more complex configurations, provided that enough degrees of freedom were used to obtain good convergence.

#### Approximate Solutions

To verify that the finite-element meshes used for the circular and elliptical crack models were sufficient to analyze cracked plates with free boundaries, through-the-thickness cracks with crack length-to-width ratios ranging from 0.2 to 0.8 were analyzed under plane strain assumptions. The meshes used here were exactly the same as those which occur on the  $\phi = \pi/2$  plane of the circular and elliptical crack models. These meshes were then used to model the center-crack tension specimen. For crack length-to-width ratios ( $c/b$ ) ranging from 0.2 to 0.6, the finite-element results were within 1.3 percent of the approximate solutions given in Reference 10. For  $c/b = 0.8$ , the finite-element result was 2 percent below the solution given in Reference 10. These results indicate that the mesh pattern along any plane has enough degrees of freedom to account for the influence of free boundaries on the stress-intensity factor.

#### Convergence

In the previous section the mesh pattern along any  $\phi = \text{constant}$  plane was found to be sufficient to account for the influence of free

boundaries even for very deep cracks. In this section, the mesh pattern in the angular direction,  $\phi$ , is studied. Figures 5 and 6 show the results of a convergence study on the stress-intensity factors for a semi-circular surface crack and a semi-elliptical surface crack, respectively, in a finite-thickness plate. The larger numbers of degrees of freedom are associated with smaller wedges in the  $\phi$ -direction and a more accurate representation of the crack shape.

For the semi-circular crack (Figure 5),  $h/a = b/a = 5$  and  $a/t = 0.8$ . This configuration was chosen because the close proximity of the back surface to the crack front was expected to cause difficulty in achieving convergence. The number of degrees of freedom ranged from 1500 to 6195. The two finest models (4317 and 6195 degrees of freedom) gave stress-intensity factors within about one percent of each other. Therefore, the model with 4317 degrees of freedom was used subsequently to obtain stress-intensity factors as a function of  $a/t$ .

Figure 6 shows the convergence study for a semi-elliptical surface crack ( $a/c = 0.2$ ). The  $h/c$  and  $b/c$  ratios were equal to four and, again,  $a/t$  was chosen as 0.8. The number of degrees of freedom ranged from 1092 to 6867. The model with 4797 degrees of freedom gave results within about one percent of those from the finest model. Therefore, the model with 4797 degrees of freedom was used subsequently to obtain stress-intensity factors and crack-opening displacements as a function of  $a/t$ .

#### Semi-Circular Surface Crack in a Finite-Thickness Plate

Figure 7 shows and Table I presents the stress-intensity factors for a semi-circular surface crack in a finite-thickness plate as a function of the parametric angle,  $\phi$ , and the crack depth-to-plate thickness ratio,  $a/t$ . Near the intersection of the crack and the free surface, the stress-intensity factor increases more rapidly with  $a/t$  than at the deepest point ( $\phi = \pi/2$ ). For each value of  $a/t$ , the stress-intensity factor calculated from the model with 4317 degrees of freedom is largest at the free surface ( $\phi = 0$ ).

For a semi-circular surface crack with  $a/t = 0.55$ , the stress-intensity factors calculated by Browning and Smith [1], who used the alternating method, were about 1 to 3 percent below the present results for various values of  $\phi$ .

#### Semi-Elliptical Surface Crack in a Finite-Thickness Plate

Figure 8 shows and Table I presents the stress-intensity factors for a semi-elliptical surface crack ( $a/c = 0.2$ ) in a finite-thickness plate as a function of the parametric angle,  $\phi$ , and the crack depth-to-plate thickness ratio,  $a/t$ . For each value of  $a/t$ , the maximum stress-intensity factor occurs at the deepest point ( $\phi = \pi/2$ ). Also, the maximum stress-intensity factor is larger for larger values of  $a/t$ .

Figures 9 and 10 show stress-intensity factors obtained by several investigators for a semi-elliptical surface crack in a finite-thickness plate. Figure 9 shows the results for a surface crack with  $a/c = 0.2$  and  $a/t = 0.8$ . Smith and Sorensen [3] and Kobayashi [2] used the

alternating method and Kathiresan [4] used the finite-element method to obtain stress-intensity factor variations along the crack front. These three solutions disagree by as much as 50 to 100 percent. The reasons for these discrepancies are not well understood. The present results, shown as solid symbols, are considerably higher than the previous solutions [2-4]. The results from Smith and Sorensen [3] are generally closer to the present results, though 10 to 25 percent lower.

Figure 10 shows a comparison of the maximum stress-intensity factors obtained by several investigators for a semi-elliptical surface crack as a function of  $a/t$ . The maximum stress-intensity factors occurred at  $\phi = \pi/2$ . The present results are shown as solid symbols. The open symbols show the results from Smith and Sorensen [3], Kobayashi [2,11], and Rice and Levy [12]. The results from Rice and Levy, obtained from a line-spring model, are about 3.5 percent below the present results over an  $a/t$  range from 0.2 to 0.6. For  $a/t > 0.6$ , the Rice-Levy solution shows a reduction in stress intensity. The dash-dot curve shows the results of an approximate equation proposed by Newman [13] for a wide range of  $a/c$  and  $a/t$  ratios. Newman's equation is within  $\pm 5$  percent of the present results over an  $a/t$  range from 0.2 to 0.8. Newman's equation gives a good engineering estimate for the maximum stress-intensity factor.

#### CONCLUDING REMARKS

A three-dimensional finite-element elastic stress analysis was used to calculate stress-intensity factor variations along the crack front for completely embedded elliptical cracks in large bodies and for semi-elliptical surface cracks (crack depth-to-crack length ratios were 0.2 and 1.0) in finite-thickness plates. Three-dimensional singularity elements were used at the crack front. A nodal force method which requires no prior assumption of either plane stress or plane strain was used to evaluate the stress-intensity factors along the crack front.

Completely embedded circular and elliptical cracks were analyzed to verify the accuracy of the finite-element analysis. The stress-intensity factors for these cracks were generally about 0.4 to 1 percent below the exact solutions. However, for the elliptical crack the calculated stress-intensity factors in the region of sharpest curvature of the ellipse were about 3 percent higher than the exact solution. The numbers of degrees of freedom in the embedded crack models were about 3000. A convergence study on stress-intensity factors for semi-elliptical surface cracks in finite-thickness plates showed that convergence was achieved for both the semi-circular and the semi-elliptical surface crack with about 4500 degrees of freedom.

For the semi-circular surface crack the maximum stress-intensity factor occurred at the intersection of the crack with the free surface. On the other hand, for the semi-elliptical surface crack (crack depth-to-crack half length ratio of 0.2), the maximum stress-intensity factor

occurred at the deepest point. For both the semi-circular and semi-elliptical surface crack the stress-intensity factors were larger for larger values of crack depth-to-plate thickness ratio.

For the semi-circular surface crack, the stress-intensity factors calculated by Browning and Smith [1] using the alternating method, agreed generally within about 3 percent with the present results. However, for semi-elliptical surface cracks (crack depth-to-plate thickness ratio of 0.2) Smith and Sorensen [3] using the alternating method gave stress-intensity factors in considerable disagreement (10 to 25 percent) with the present results. For semi-elliptical surface cracks the results from Rice and Levy [12] for crack depth-to-plate thickness ratios less than or equal to 0.6 and an approximate equation proposed by Newman [13] were in good agreement with the present results.

The stress-intensity factors obtained herein should be useful in correlating fatigue crack-growth rates as well as fracture toughness calculations for the surface-crack configuration considered.

REFERENCES

- [1] Browning, W.M. and Smith, F.W.: "An Analysis for Complex Three-Dimensional Crack Problems," Developments in Theoretical and Applied Mechanics, Vol. 8, Proceedings of the 8th SECTAM Conference, April 1976.
- [2] Kobayashi, A.S.: "Surface Flaws in Plates in Bending," Proceedings of the 11th Annual Meeting of the Society of Engineering Science, Austin, Texas, October 1975.
- [3] Smith, F.W. and Sorensen, D.R.: "Mixed Mode Stress Intensity Factors for Semi-Elliptical Surface Cracks," NASA CR-134684, June 1974.
- [4] Kathiresan, K.: "Three-Dimensional Linear Elastic Fracture Mechanics Analysis by a Displacement Hybrid Finite Element Model." Ph.D. Thesis, Georgia Institute of Technology, September 1976.
- [5] Green, A.E. and Sneddon, I.N.: "The Distribution of Stress in the Neighborhood of a Flat Elliptical Crack in an Elastic Solid," Proc. Cambridge Phil. Soc., 46, 1959.
- [6] Tracey, D.M.: "Finite Element for Three-Dimensional Elastic Crack Analysis," Nucl. Engr. and Design, Vol. 26, 1974.
- [7] Barsoum, R.S.: "On the Use of Isoparametric Finite Elements in Linear Fracture Mechanics," Int. J. Num. Meth. Engr., Vol. 10, no. 1, January 1976.
- [8] Muri, S. and Kathiresan, A.: "An Assumed Displacement Hybrid Finite Element Model for Three-Dimensional Linear Fracture Mechanics Analysis," Proc. 12th Annual Meeting of the Soc. Engr. Science, University of Texas, Austin, Texas, October 1975.

- [9] Raju, I.S. and Newman, J.C., Jr.: "Three-Dimensional Finite-Element Analysis of Finite-Thickness Fracture Specimens," NASA TN D-8414, 1977.
  
- [10] Tada, H.; Paris, P.C.; and Irwin, G.R.: "The Stress Analysis of Cracks Handbook," Del. Research Corp., C. 1973, pg. 28.1.
  
- [11] Kobayashi, A.S.: "Crack Opening Displacement in a Surface Flawed Plate Subjected to Tension or Plate Bending," presented at the Second International Conference on Mechanical Behavior of Materials, Boston, Mass., August 1976.
  
- [12] Rice, J.R. and Levy, N.: "The Part- Through Surface Crack in an Elastic Plate," Trans. ASME. J. Appl. Mech. Paper No. 71-APM-20, 1970.
  
- [13] Newman, J.C., Jr.: "Fracture Analysis of Surface- and Through-Cracked Sheets and Plates," Engineering Fracture Mechanics, Vol. 5, 1973.

**TABLE I: Boundary Correction Factors,  $F$ , for Semi-Elliptical Surface Cracks Subjected to tension**

$$(\nu = 0.3; F = K/S \sqrt{\pi a/Q})$$

| a/c              | $2\phi/\pi$ | a/t   |       |       |       |
|------------------|-------------|-------|-------|-------|-------|
|                  |             | 0.2   | 0.4   | 0.6   | 0.8   |
| 1 <sup>a</sup>   | 0           | 1.166 | 1.229 | 1.355 | 1.464 |
|                  | 0.125       | 1.130 | 1.206 | 1.321 | 1.410 |
|                  | 0.25        | 1.092 | 1.157 | 1.256 | 1.314 |
|                  | 0.375       | 1.070 | 1.126 | 1.214 | 1.234 |
|                  | 0.5         | 1.054 | 1.104 | 1.181 | 1.193 |
|                  | 0.625       | 1.046 | 1.088 | 1.153 | 1.150 |
|                  | 0.75        | 1.039 | 1.075 | 1.129 | 1.134 |
|                  | 0.875       | 1.037 | 1.066 | 1.113 | 1.118 |
|                  | 1.0         | 1.036 | 1.062 | 1.107 | 1.112 |
| 0.2 <sup>b</sup> | 0           | 0.608 | 0.724 | 0.899 | 1.190 |
|                  | 0.125       | 0.632 | 0.775 | 0.953 | 1.217 |
|                  | 0.25        | 0.738 | 0.883 | 1.080 | 1.345 |
|                  | 0.375       | 0.863 | 1.009 | 1.237 | 1.504 |
|                  | 0.5         | 0.968 | 1.122 | 1.384 | 1.657 |
|                  | 0.625       | 1.046 | 1.222 | 1.501 | 1.759 |
|                  | 0.75        | 1.099 | 1.297 | 1.581 | 1.824 |
|                  | 0.875       | 1.130 | 1.344 | 1.627 | 1.846 |
|                  | 1.0         | 1.140 | 1.359 | 1.642 | 1.851 |

<sup>a</sup>  $h/c = b/c = 5.0;$

<sup>b</sup>  $h/c = b/c = 4.0$

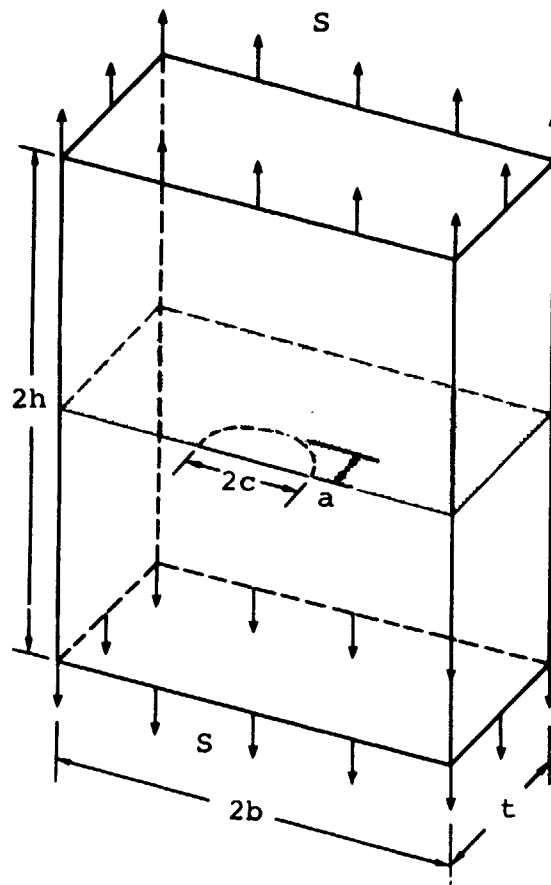


Fig. 1.- Surface crack in a plate subjected to tension.

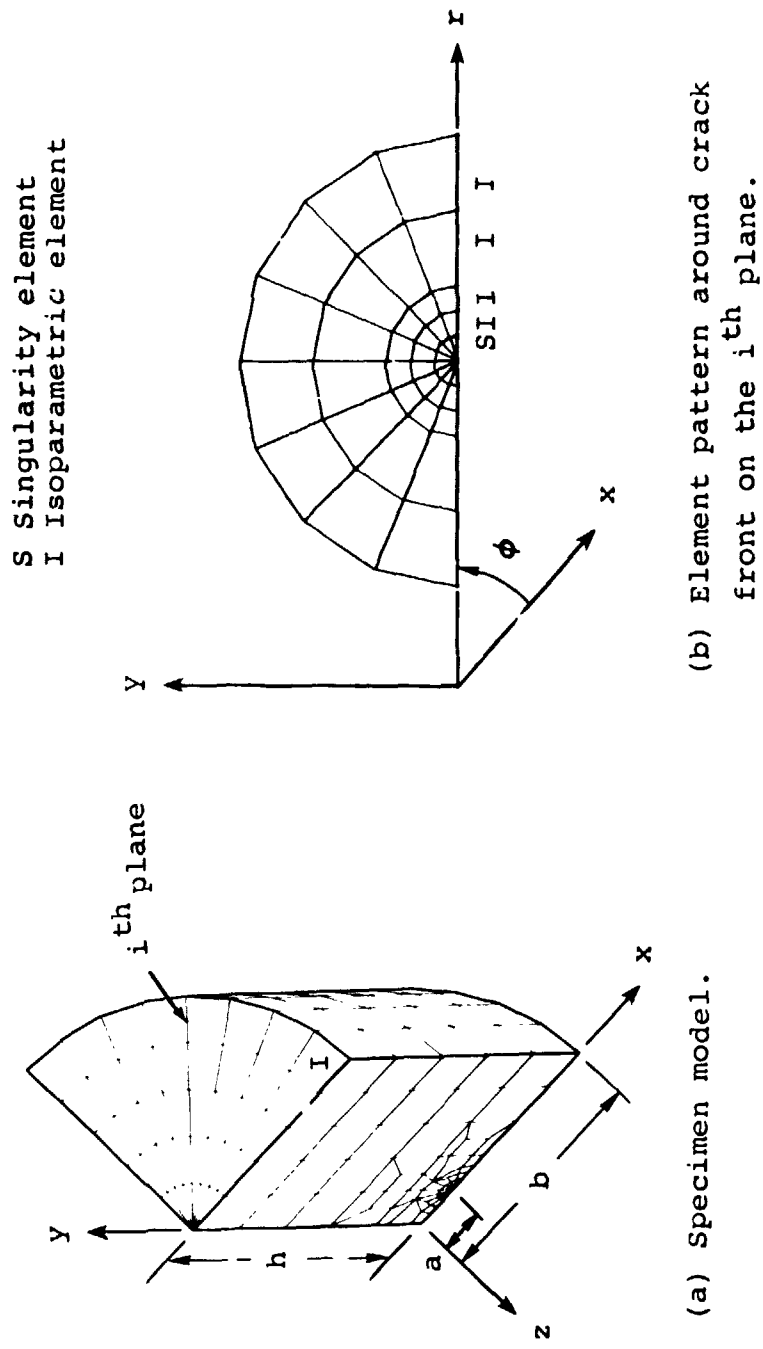
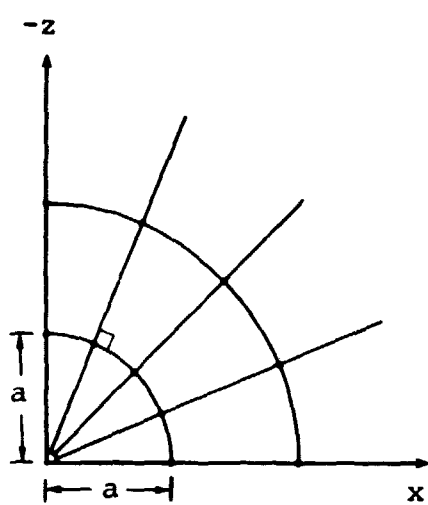
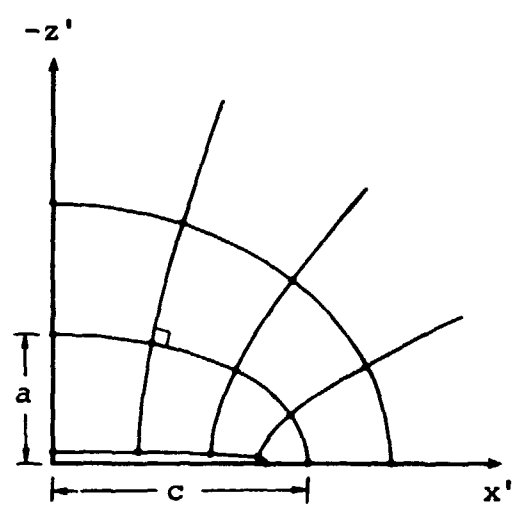


Fig. 2.- Finite-element idealization for an embedded circular (penny-shaped) crack.

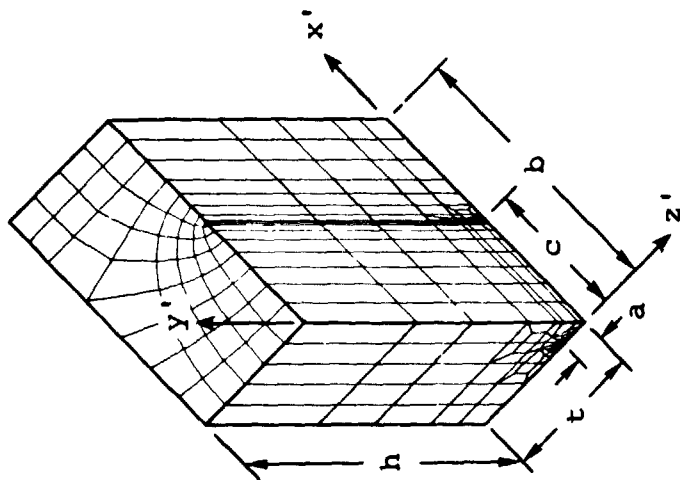


(a) Circular crack.

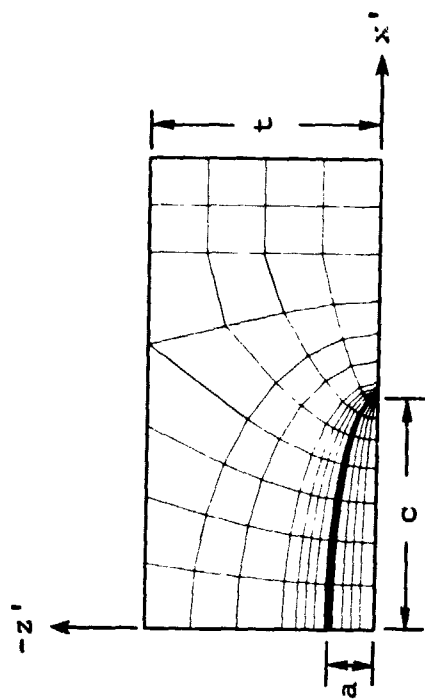


(b) Elliptic crack.

Fig. 3.- Circle to ellipse transformation.



(a) Specimen model.



(b) Element pattern on  $y' = 0$  plane.

Fig. 4.- Finite-element idealization for a semi-elliptical surface crack.

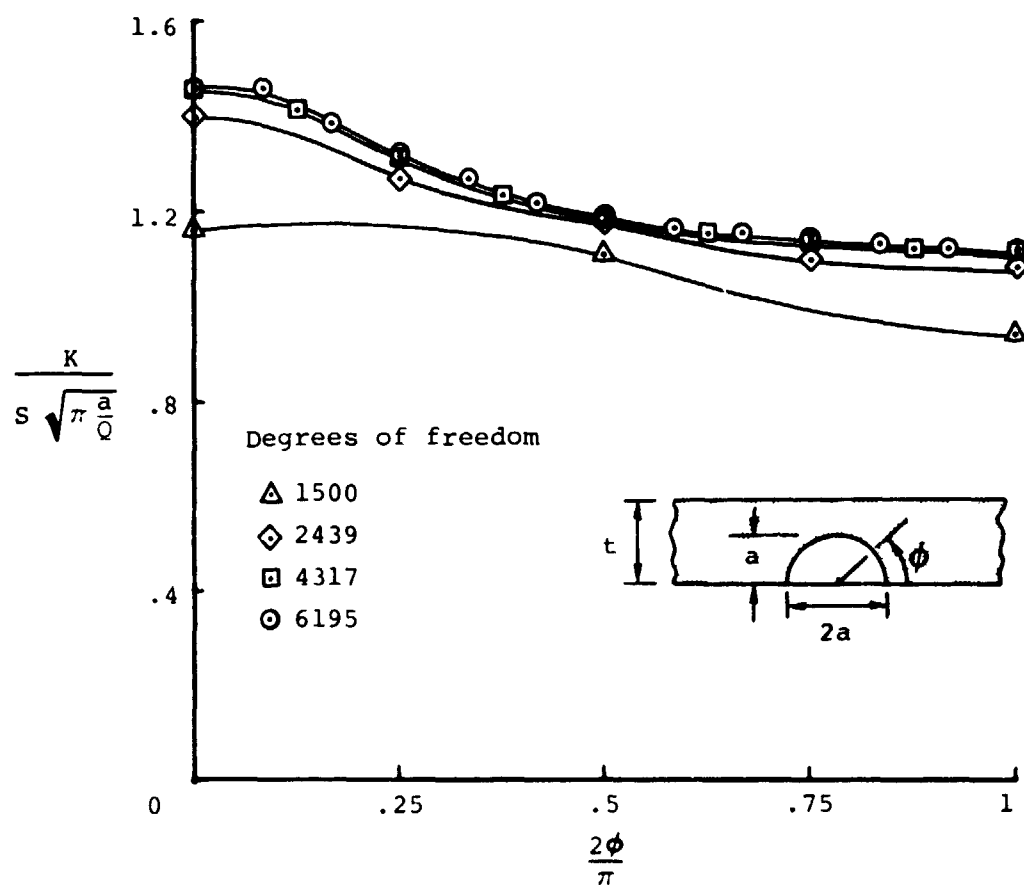


Fig. 5.- Convergence of stress-intensity factors for a deep semi-circular surface crack ( $Q = \pi^2/4$ ).

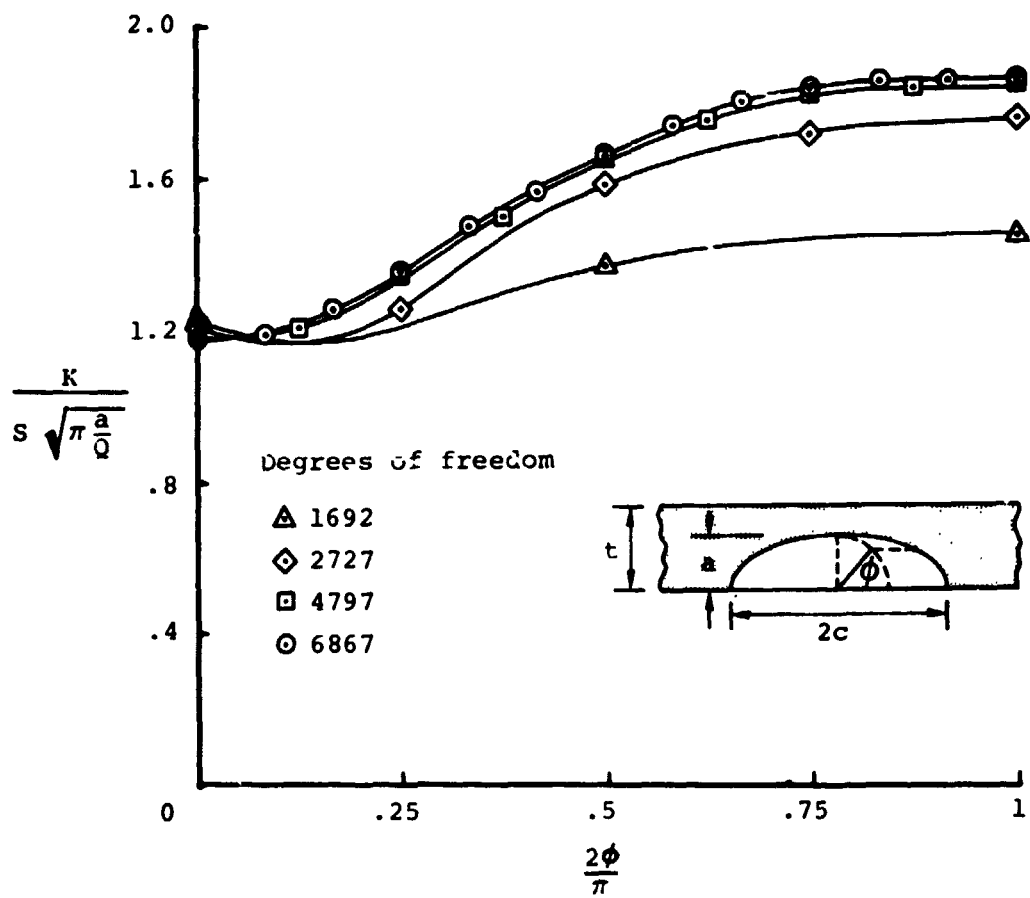


Fig. 6.- Convergence of stress-intensity factors for a deep semi-elliptical surface crack ( $Q = 1.104$ ;  $a/t = 0.8$ ;  $a/c = 0.2$ ).

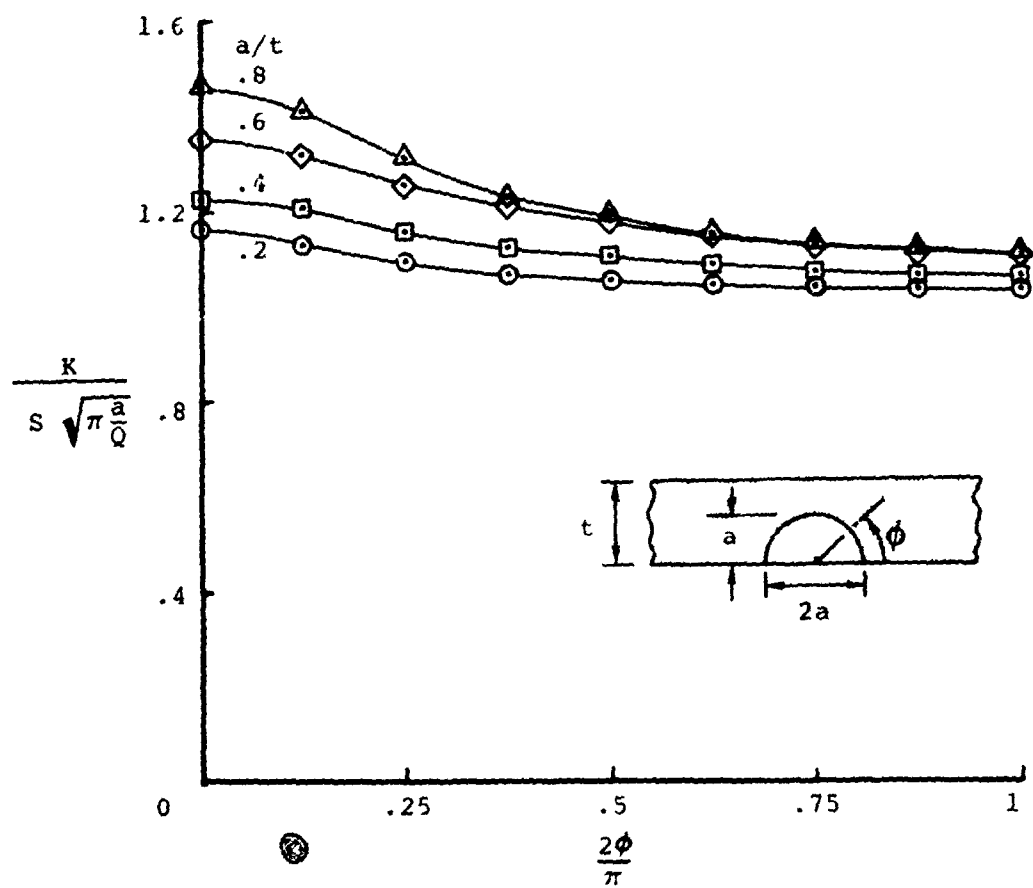


Fig. 7.- Distribution of stress-intensity factors along crack front for a semi-circular surface crack ( $Q = \pi^2/4$ ).

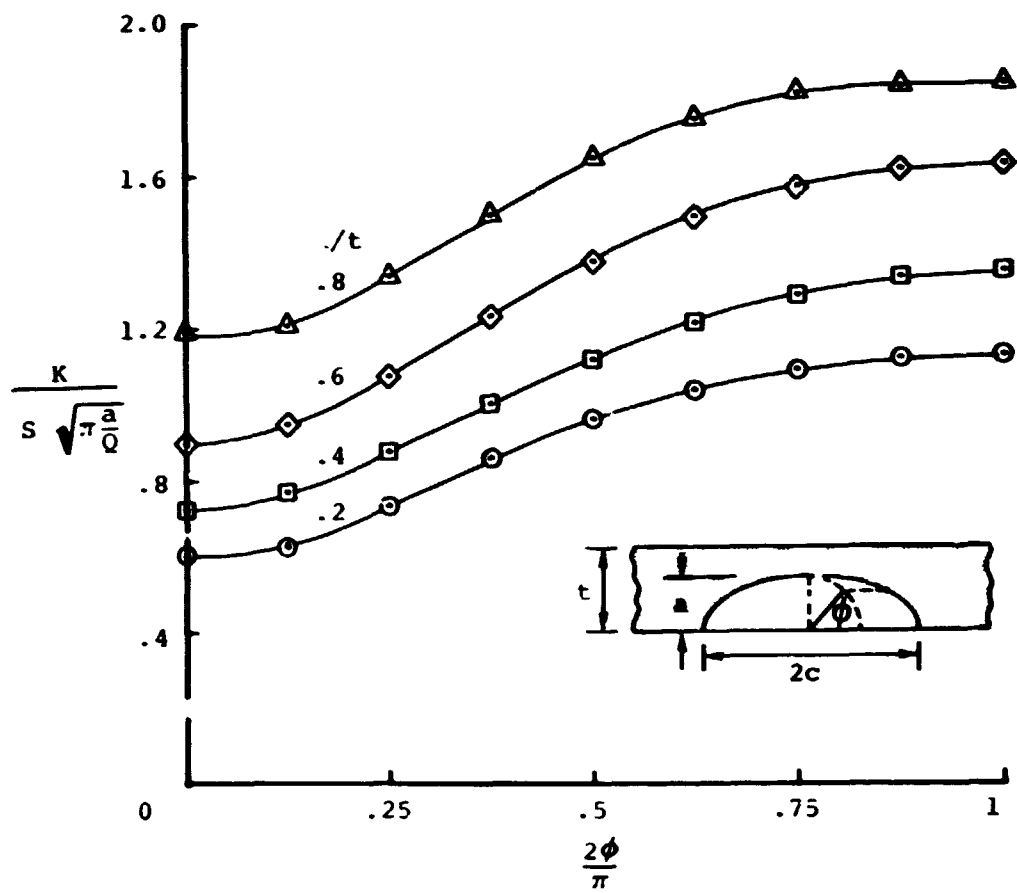


Fig. 8.- Distribution of stress-intensity factors along crack front for a semi-elliptical surface crack ( $Q = 1.104$ ;  $a/c = 0.2$ ).

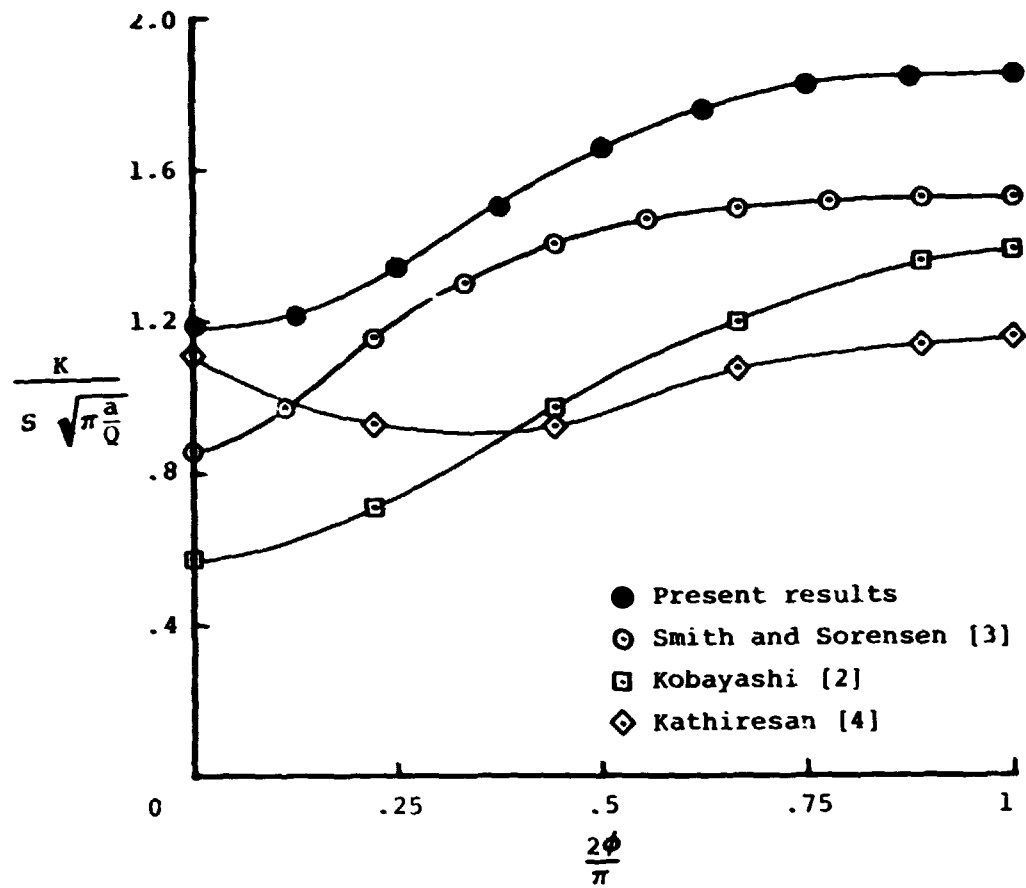


Fig. 9.- Comparison of stress-intensity factors for a deep semi-elliptical surface crack ( $Q = 1.104$ ;  $a/t = 0.8$ ;  $a/c = 0.2$ ).

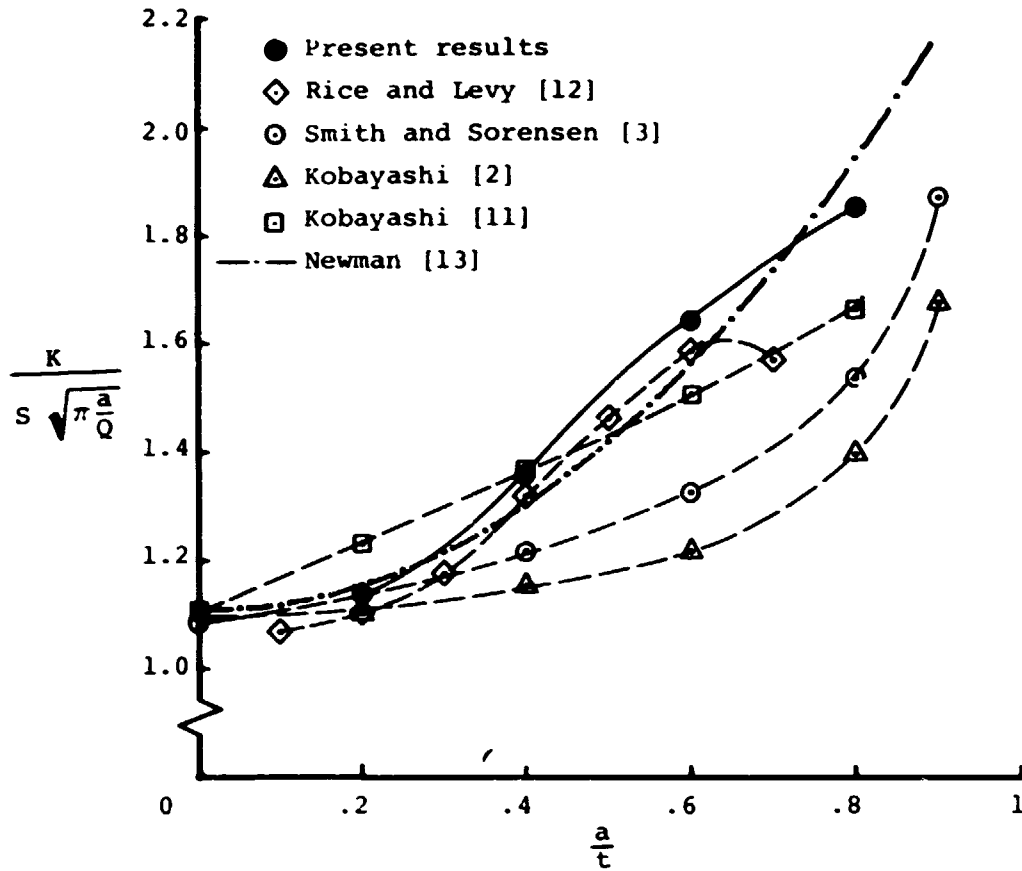


Fig. 10.- Comparison of the maximum stress-intensity factor for a semi-elliptical surface crack as a function of  $a/t$  ( $\phi = \pi/2$ ;  $Q = 1.104$ ;  $a/c = 0.2$ ).